α-Propargyl Amino Acid-Derived Optically Active Novel Substituted Polyacetylenes: Synthesis, Secondary Structures, and Responsiveness to Ions

Hiromitsu Sogawa, Masashi Shiotsuki,* Fumio Sanda

Department of Polymer Chemistry, Graduate School of Engineering, Kyoto University, Katsura Campus, Nishikyo-ku, Kyoto 615-8510, Japan
Correspondence to: F. Sanda (E-mail: sanda.fumio.5n@kyoto-u.ac.jp)

Received 13 October 2011; accepted 30 January 2012; published online 5 March 2012
DOI: 10.1002/pola.25975

ABSTRACT: Novel optically active substituted acetylenes HC≡$CCH_2CR^1(CO_2CH_3)NHR^2$ [(*S*)-/(*R*)-**1**: R^1 = H, R^2 = Boc, (*S*)-**2**: R^1 = CH_3, R^2 = Boc, (*S*)-**3**: R^1 = H, R^2 = Fmoc, (*S*)-**4**: R^1 = CH_3, R^2 = Fmoc (Boc = *tert*-butoxycarbonyl, Fmoc = 9-fluorenylmethoxycarbonyl)] were synthesized from α-propargylglycine and α-propargylalanine, and polymerized with a rhodium catalyst to provide the polymers with number-average molecular weights of 2400–38,900 in good yields. Polarimetric, circular dichroism (CD), and UV–vis spectroscopic analyses indicated that poly[(*S*)-**1**], poly[(*R*)-**1**], and poly[(*S*)-**4**] formed predominantly one-handed helical structures both in polar and nonpolar solvents. Poly[(*S*)-**1a**] carrying unprotected carboxy groups was obtained by alkaline hydrolysis of poly[(*S*)-**1**], and poly[(*S*)-**4b**] carrying unprotected amino groups was obtained by removal of Fmoc groups of poly[(*S*)-**4**] using piperidine. Poly[(*S*)-**1a**] and poly[(*S*)-**4b**] also exhibited clear CD signals, which were different from those of the precursors, poly[(*S*)-**1**] and poly[(*S*)-**4**]. The solution-state IR measurement revealed the presence of intramolecular hydrogen bonding between the carbamate groups of poly[(*S*)-**1**] and poly[(*S*)-**1a**]. The plus CD signal of poly[(*S*)-**1a**] turned into minus one on addition of alkali hydroxides and tetrabutylammonium fluoride, accompanying the red-shift of λ_{max}. The degree of λ_{max} shift became large as the size of cation of the additive. © 2012 Wiley Periodicals, Inc. J Polym Sci Part A: Polym Chem 50: 2008–2018, 2012

KEYWORDS: chiral; conjugated polymers; conformational analysis; polyacetylenes; stimuli-sensitve polymers

INTRODUCTION The helix is one of the most common higher-order structures of macromolecules. Many sophisticated and intricate functions of biomacromolecules such as proteins and DNA largely depend on their well-defined helical structures. Various types of helical polymers have been synthesized so far including polymethacrylates,[1] polyisocyanides,[2] polysilanes,[3] poly(phenyleneethynylene)s,[4] and polyacetylenes,[5] dating back to the discovery of isotactic polypropylene by Natta et al.[6] Monosubstituted polyacetylenes synthesized by the polymerization with rhodium catalysts feature a highly *cis*-stereoregurlar structure.[7–9] Introduction of appropriate chiral substituents into the side chain leads to the formation of a helical structure with predominantly one-handed screw sense. We have reported that rhodium-based *cis*-stereoregular polyacetylene derivatives such as poly(*N*-propargylamide)s,[10–12] poly(*N*-propargylcarbamate)s,[13,14] poly(*N*-butynylamide)s,[15,16] poly(1-methylpropargyl-*N*-alkylcarbamate)s[17] form helical structures with predominantly one-handed screw sense, which are stabilized by intramolecular hydrogen bonds together with the steric repulsion between the side chains in the biomimetically same way as peptides and proteins. They undergo reversible helix–helix or helix–coil transitions by external stimuli such as heat and the addition of polar solvents, wherein the formation and deformation of hydrogen bonds are key factors for the conformational transition.

Amino acid is a useful chiral building block for synthetic helical polymers, because the amino and carboxy groups are transformable into wide variety of functional groups, making versatile molecular design possible. When amide groups are introduced in amino acid-based helical polymers, they are usable for stabilizing the helical structure due to the strong nature of forming hydrogen bonding in a manner similar to α-helix of peptide. Various helical polyacetylenes functionalized with amino acids have been also synthesized so far,[18–42] some of which change the conformation according to external stimuli such as temperature,[18,19] solvent,[20–23] acid/base,[24–27] electricity,[28] and photo-irradiation.[29,30] Amino

**Present address:* Molecular Engineering Institute, Kinki University, Kayanomori, Iizuka, Fukuoka 820-8555, Japan.

Additional Supporting Information may be found in the online version of this article.

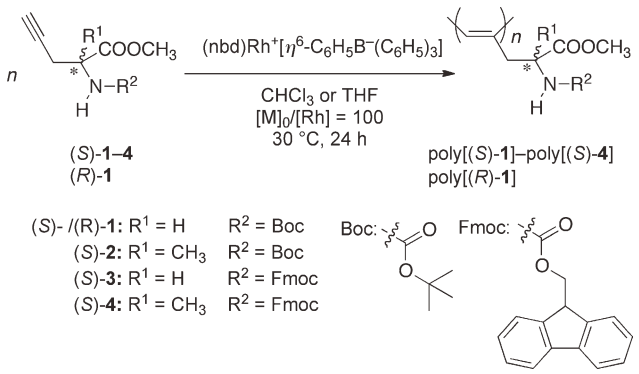

SCHEME 1 Polymerization of monomers (*S*)-/(*R*)-**1**–**4**.

acid-based helical polymers also show useful properties including chemical sensing,[31–34] chiral recognition,[35] and asymmetric induction[36–39] originated from the conjugated backbone and regularly ordered functional groups at the side chain strands.

Recently, the synthesis of highly optically pure non-natural amino acids becomes possible by the enantioselective alkylation of a prochiral protected glycine derivative utilizing a chiral phase transfer catalyst (Maruoka catalyst) having binaphthyl group.[43] Various optically active amino acids bearing olefinic pendants are now commercially synthesized with Maruoka catalyst, and find application to hydrocarbon stapling (ring-closing metathesis reaction) of helical peptides, which provides a useful strategy for experimental and therapeutic modulation of protein–protein interactions in many signaling pathways.[44] Non-natural optically active amino acids bearing acetylenic pendants such as α-propargylglycine are synthesized by Maruoka catalyst as well. In the course of our study on amino acid-based helical polyacetylenes, we have decided to utilize α-propargyl amino acid derivatives as the monomers. The present article deals with the synthesis of novel polyacetylenes from α-propargylglycine and alanine (Scheme 1), and examination of the secondary structures. As far as we know, this is the first example regarding the synthesis of α-propargyl amino acid-derived helical polyacetylenes. We further disclose the removal of protecting groups from the amino and carboxy groups, and ion-responsiveness of the polymers having unprotected amino/carboxy groups.

EXPERIMENTAL

Measurements

^{1}H (400 MHz) and ^{13}C (100 MHz) NMR spectra were recorded on a JEOL EX-400 or a JEOL AL-400 spectrometer. IR spectra were measured on a JASCO FT/IR-4100 spectrophotometer. Melting points (mp) were measured on a Yanaco micro melting point apparatus. Mass spectra were measured on a Thermo Scientific Exactive mass spectrometer. Specific rotations ($[\alpha]_D$) were measured on a JASCO DIP-1000 digital polarimeter. Number- and weight-average molecular weights (M_n and M_w) of polymers were determined by size-exclusion column chromatography (SEC, Shodex columns KF805 × 3) eluted with tetrahydrofuran (THF) calibrated by polystyrene standards at 40 °C. CD and UV–vis absorption spectra were recorded on a JASCO J-820 spectropolarimeter.

Materials

Unless stated otherwise, reagents and solvents were purchased and used without purification. (nbd)Rh$^+$[η^6-$C_6H_5B^-(C_6H_5)_3$] (nbd = 2,5-norbornadiene) was prepared according to the literature.[45] α-Propargyl amino acid derivatives [(*S*)-α-propargylglycine, (*R*)-α-propargylglycine, (*S*)-α-propargylalanine, (*S*)-*N*-Fmoc-α-propargylalanine (Fmoc = 9-fluorenylmethoxycarbonyl) (*ee* ≥ 99%)] and di-*tert*-butylcarbonate [$(Boc)_2O$] (Boc = *tert*-butoxycarbonyl) were gifted from Nagase & Co., LTD. and Tokuyama. $CHCl_3$, THF, and *N,N*-dimethylformamide (DMF) used for polymerization were distilled prior to use.

Monomer Synthesis

(S)-N-Boc-α-propargylglycine Methyl Ester [(S)-1]

$(Boc)_2O$ (3.72 g, 15.0 mmol) and K_2CO_3 (1.59 g, 15.0 mmol) were added to a solution of (*S*)-α-propargylglycine (1.13 g, 10.0 mmol) in 1,4-dioxane/H_2O (30 mL/50 mL) at 0 °C, and the resulting mixture was stirred at room temperature overnight. 1,4-Dioxane was evaporated off, and the residual solution was carefully acidified with 0.5 M HCl to pH = 3. The resulting solution was extracted with CH_2Cl_2. The organic layer was washed with water and saturated NaCl aq., dried over anhydrous $MgSO_4$, and then filtered. The filtrate was concentrated to obtain (*S*)-*N*-Boc-α-propargylglycine [(*S*)-**1a**] as a viscosity liquid. After that, 1-(3-dimethylaminopropyl)-3-ethylcarbodiimide hydrochloride (EDC•HCl, 2.30 g, 12.0 mmol), *N,N*-dimethyl-4-aminopyridine (DMAP, 0.140 g, 1.20 mmol), and MeOH (2.00 mL, 49.4 mmol) were added to a solution of (*S*)-**1a** in CH_2Cl_2 (40 mL) at 0 °C, and then the resulting mixture was stirred at room temperature overnight. It was washed with 1.0 M HCl, saturated $NaHCO_3$ aq., and saturated NaCl aq., dried over anhydrous $MgSO_4$, and then filtered. The filtrate was concentrated, and the residual mass was purified by preparative HPLC to obtain (*S*)-**1** as a viscous liquid in 44%. $[\alpha]_D$ +23° (*c* = 0.14 g/dL, THF). IR (in $CHCl_3$): 3436, 3308, 2982, 1746, 1709, 1502, 1368, 1222, 1162, 1064, 655 cm^{-1}. ^{1}H NMR (400 MHz, $CDCl_3$): δ 1.45 [s, 9H, —C(CH_3)$_3$], 2.07 (t, *J* = 2.4 Hz, 1H, —C≡C*H*), 2.71–2.74 (m, 2H, —CH_2—), 3.78 (s, 3H, —OCH_3), 4.45–4.50 (m, 1H, —C*H*—), 5.45 (d, *J* = 8.4 Hz, 1H, —N*H*—). ^{13}C NMR (100 MHz, $CDCl_3$): δ 22.56 (—CH_2—), 28.06 [—C(CH_3)$_3$], 51.76 (—OCH_3), 52.38 (—*C*H—), 71.46 (—C≡*C*H), 78.38 (—*C*≡CH), 79.89 [—*C*(CH_3)$_3$], 154.89 (—NH*C*O—), 170.93 (—*C*OOCH$_3$). High-resolution mass spectra (HRMS, *m*/*z*): [M + Na]$^+$ calcd for $C_{11}H_{17}NO_4Na$, 250.1055; found, 250.1042.

(R)-N-Boc-α-propargylglycine Methyl Ester [(R)-1]

The title compound was synthesized from (*R*)-α-propargylglycine in a manner similar to (*S*)-**1**. Yield 43% (viscous liquid). $[\alpha]_D$ −21° (*c* = 0.09 g/dL, THF). IR (in $CHCl_3$): 3436, 3308, 3019, 2981, 2123, 1747, 1709, 1503, 1368, 1215, 1162, 1064, 668 cm^{-1}. ^{1}H NMR (400 MHz, $CDCl_3$): δ 1.45 [s, 9H, —C(CH_3)$_3$], 2.07 (t, *J* = 2.8 Hz, 1H, —C≡C*H*), 2.71–2.74 (m, 2H, —CH_2—), 3.78 (s, 3H, —OCH_3), 4.44–4.50 (m, 1H, —C*H*—), 5.44 (d, *J* = 8.4 Hz, 1H, —N*H*—). ^{13}C NMR (100

MHz, $CDCl_3$): δ 22.56 (—CH_2—), 28.07 [—C(CH_3)$_3$], 51.78 (—OCH_3), 52.37 (—CH—), 71.45 (—C≡CH), 78.39 (—C≡CH), 79.89 [—C(CH_3)$_3$], 154.89 (—NHCO—), 170.92 (—COOCH$_3$). HRMS. (m/z): [M + Na]$^+$ calcd for $C_{11}H_{17}NO_4Na$, 250.1055; found, 250.1050.

(S)*-N-*Boc*-α-*propargylalanine Methyl Ester [(S)-2]

The title compound was synthesized from (*S*)-α-propargylalanine in a manner similar to (*S*)-**1**. Yield 38% (white solid). Mp 72–73 °C. $[\alpha]_D$ −63° (c = 0.10 g/dL, THF). IR (KBr): 3382, 3331, 3318, 2985, 2937, 2120, 1732, 1711, 1666, 1517, 1457, 1385, 1251, 1174, 1064, 624 cm^{-1}. ^{1}H NMR (400 MHz, $CDCl_3$): δ 1.43 [s, 9H, —C(CH_3)$_3$], 1.54 [s, 3H, —CH_3], 2.06 (t, J = 2.4 Hz, 1H, —C≡CH), 2.88–2.96 (m, 2H, —CH_2—), 3.76 (s, 3H, —OCH_3), 5.37 (br, 1H, —NH—). ^{13}C NMR (100 MHz, $CDCl_3$): δ 22.93 (—CH_3), 26.69 (—CH_2—), 28.04 [—C(CH_3)$_3$], 52.45 (—OCH_3), 57.97 (—CH—), 71.08 (—C—CH), 79.20 [—C(CH_3)$_3$], 79.66 (—C—CH), 154.16 (—NHCO—), 173.41 (—COOCH$_3$). HRMS. (m/z): [M + H]$^+$ calcd for $C_{12}H_{20}NO_4$, 242.1392; found, 242.1386.

(S)*-N-*Fmoc*-α-*propargylglycine Methyl Ester [(S)-3]

A solution of *N*-Fmoc-succinimide (1.01 g, 3.00 mmol) in 1,2-dimethoxyethane (DME) (10 mL) was added to a solution of (*S*)-α-propargylglycine (0.226 g, 2.00 mmol) in 10 wt % Na_2CO_3 aq. (10 mL) at 0 °C, and the resulting mixture was stirred at room temperature overnight. Precipitates formed were filtered off, and then DME was removed from the filtrate by evaporation. The residual solution was carefully acidified by 0.1 M HCl to adjust the pH neutral, and then extracted with EtOAc. The organic phase was washed with 0.1 M HCl, and saturated NaCl aq., dried over anhydrous $MgSO_4$, and then filtered. The filtrate was concentrated to obtain (*S*)-*N*-Fmoc-α-propargylglycine [(*S*)-**3a**]. After that, (*S*)-**3** was synthesized from (*S*)-**3a** and MeOH in a manner similar to (*S*)-**1**, and purified by silica gel column chromatography eluted with hexane/$CHCl_3$ = 1/1 (v/v). Yield 32% (white solid). Mp 136–137 °C. $[\alpha]_D$ −9° (c = 0.08 g/dL, THF). IR (KBr): 3320, 3273, 3065, 3020, 2951, 2116, 1734, 1691, 1543, 1450, 1296, 1014, 746 cm^{-1}. ^{1}H NMR (400 MHz, $CDCl_3$): δ 2.05 (s, 1H, —C≡CH), 2.75–2.78 (m, 2H, —CH_2—), 3.75 (s, 3H, —OCH_3), 4.21 (t, J = 6.8 Hz, 1H, >CH—), 4.38 (d, J = 7.2 Hz, 2H, —CH_2O—), 4.53–4.55 (m, 1H, —CH—), 5.74 (d, J = 6.8 Hz, 1H, —NH—), 7.28 (t, J = 7.6 Hz, 2H, Ar), 7.37 (t, J = 7.6 Hz, 2H, Ar), 7.59 (d, J = 6.8 Hz, 2H, Ar), 7.73 (d, J = 7.6 Hz, 2H, Ar). ^{13}C NMR (100 MHz, $CDCl_3$): δ 22.56 (—CH_2—), 46.93 (>CH—), 52.23 (—OCH_3), 52.26 (—CH—), 67.08 (—CH_2O—), 71.74 (—C≡CH), 78.21 (—C≡CH), 119.86, 124.97, 126.93, 127.59, 141.13, 143.57 (Ar), 155.50 (—NHCO—), 170.64 (—COOCH$_3$). HRMS. (m/z): [M + Na]$^+$ calcd for $C_{21}H_{19}NO_4Na$, 372.1212; found, 372.1207.

(S)*-N-*Fmoc*-α-*propargylalanine Methyl Ester [(S)-4]

The title compound was synthesized from (*S*)-*N*-Fmoc-α-propargylalanine containing 27% of methyl *tert*-butyl ether and MeOH in a manner similar to (*S*)-**1**, and purified by silica gel column chromatography eluted with hexane/$CHCl_3$ = 1/1 (v/v). Yield 53% (white solid). Mp 54–56 °C. $[\alpha]_D$ −45° (c = 0.09 g/dL, THF). IR (KBr): 3357, 3292, 3065, 3040, 2951, 2120, 1719, 1524, 1509, 1450, 1276, 1231, 1118, 1077, 974, 739 cm^{-1}. ^{1}H NMR (400 MHz, $CDCl_3$): δ 1.57 (s, 3H, —CH_3), 2.01 (s, 1H, —C≡CH), 2.89–3.05 (m, 2H, —CH_2—), 3.73 (s, 3H, —OCH_3), 4.20 (t, J = 6.8 Hz, 1H, >CH—), 4.38 (br, 2H, —CH_2O—), 5.76 (br, 1H, —NH—), 7.27 (t, J = 7.6 Hz, 2H, Ar), 7.35 (t, J = 7.2 Hz, 2H, Ar), 7.57 (d, J = 7.2 Hz, 2H, Ar), 7.71 (d, J = 7.6 Hz, 2H, Ar). ^{13}C NMR (100 MHz, $CDCl_3$): δ 23.03 (—CH_3), 26.73 (—CH_2—), 47.02 (>CH—), 52.78 (—OCH_3), 58.52 (—CH—), 66.57 (—CH_2O—), 71.25 (—C≡CH), 79.08 (—C≡CH), 119.74, 124.85, 126.81, 127.44, 141.04, 143.56 (Ar), 154.46 (—NHCO—), 172.96 (—COOCH$_3$). HRMS. (m/z): [M + H]$^+$ calcd for $C_{22}H_{22}NO_4$, 364.1549; found, 364.1532.

Polymerization

All the polymerizations were carried out in a glass tube equipped with a three-way stopcock under nitrogen. A typical experimental procedure for polymerization is given below.

A solution of (nbd)Rh$^+$[η^6-$C_6H_5B^-(C_6H_5)_3$] (5.1 mg, 10 μmol) in $CHCl_3$ (2.5 mL) was added to a solution of a monomer (1.0 mmol) in $CHCl_3$ (2.5 mL) under dry nitrogen, and the resulting solution was kept at 30 °C for 24 h. The reaction mixture was poured into a large amount of hexane to precipitate a polymer. It was separated by filtration using a membrane filter (ADVANTEC H100A047A) and dried under reduced pressure.

Alkaline Hydrolysis of Ester Groups of Poly[(*S*)-1]

Aqueous NaOH (1.00 M, 1.00 mL) was added to a solution of poly[(*S*)-**1**] (0.113 g, 0.500 unit mmol) in THF/MeOH/H_2O (5 mL/5 mL/10 mL) at room temperature, and then the resulting mixture was stirred at 60 °C for 8 h. THF and MeOH were evaporated from the mixture, and the residual solution was carefully acidified by citric acid, and then extracted with EtOAc. The organic phase was washed with saturated NaCl aq., and then dried over anhydrous $MgSO_4$. EtOAc was evaporated off to obtain poly[(*S*)-**1a**] as a yellow solid in 76%. $[\alpha]_D$ +245° (c = 0.07 g/dL, THF).

Removal of Fmoc Groups from Poly[(*S*)-4]

Piperidine (2.00 mL) was added to a solution of poly[(*S*)-**4**] (0.108 g, 0.300 unit mmol) in $CHCl_3$ (10.0 mL). The resulting mixture was stirred at room temperature for 8 h, and then poured into hexane to precipitate the produced polymer. It was collected by filtration using a membrane filter (ADVANTECH H100A047A) and dried under reduced pressure to obtain poly[(*S*)-**4b**] as a yellow solid in 83%.

Methyl Esterification of Poly[(*S*)-1a]

A solution of trimethylsilyldiazomethane in hexane (0.6 M, 1.0 mL) was added to a solution of poly[(*S*)-**1a**] (0.010 mg, 0.027 unit mmol) in THF/MeOH (5 mL/5 mL). The resulting mixture was stirred at room temperature for 6 h, and then concentrated to obtain methyl esterificated poly[(*S*)-**1a**]. $[\alpha]_D$ +107° (c = 0.09 g/dL, THF). The ^{1}H NMR spectroscopic data were almost the same as those of poly[(*S*)-**1**].

TABLE 1 Polymerization of (*S*)-/(*R*)-**1**–**4**[a]

		Polymer			
Run	Monomer	Yield[b] (%)	M_n[c]	M_w/M_n[c]	$[\alpha]_D$[d] (°)
1	(*S*)-**1**	83	38,900	1.9	+113
2	(*R*)-**1**	76	30,700	1.8	−106
3	(*S*)-**2**	–[e]	–[e]	–[e]	–[e]
4	(*S*)-**3**	–[e]	–[e]	–[e]	–[e]
5	(*S*)-**4**	61	2,400	1.6	–[f]
6[g]	(*S*)-**4**	83	7,900	1.7	+662

[a] Conditions: catalyst (nbd)Rh$^+$[η^6-$C_6H_5B^-(C_6H_5)_3$], nbd = 2,5-norbornadiene, $[M]_0$ = 0.20 M, $[M]_0$/[Rh] = 100, in $CHCl_3$, at 30 °C for 24 h.
[b] Hexane-insoluble part {poly[(*S*)-**1**] and poly[(*R*)-**1**]} and Et_2O-insoluble part {poly[(*S*)-**4**]}.
[c] Determined by SEC eluted with THF, polystyrene calibration.
[d] Measured by polarimetry at room temperature, c = 0.09–0.14 g/dL in THF. $[\alpha]_D$ of monomers: (*S*)-**1**, +23°; (*R*)-**1**, −22°; (*S*)-**4**, −45°.
[e] Not determined due to insolubility.
[f] Not determined.
[g] $[M]_0$ = 0.50 M, in THF. Gelation occurred at this concentration in $CHCl_3$.

Addition of Alkali Hydroxides and TBAF to Poly[(*S*)-1]

A solution of an alkali hydroxide or tetrabutylammonium fluoride (TBAF) in THF, MeOH, or H_2O (5.0 mL, 0.25–4.0 mM) was added to a solution of poly[(*S*)-**1a**] in THF or MeOH (5.0 mL, 1.0 mM). The CD and UV–vis spectra of the resulting mixture were measured. Alkali hydroxides and TBAF were used as purchased from commercial suppliers.

Spectroscopic Data of the Polymers Poly[(*S*)-1]

IR (KBr): 3368, 2978, 2933, 1747, 1717, 1509, 1367, 1166, 1057, 1024, 860, 781 cm^{-1}. ^{1}H NMR (400 MHz, $CDCl_3$): δ 1.42 [br, 9H, $(CH_3)_3C$—], 2.71 (br, 2H, —CH_2—), 3.70 (br, 3H, —OCH_3), 4.30 (br, 1H, —*CH*—), 5.50–6.64 (br, 2H, —C=C*H*—, —N*H*—). **Poly[(*R*)-1]**: IR (KBr): 3368, 2978, 2933, 1746, 1718, 1509, 1366, 1167, 1057, 1024, 856, 781 cm^{-1}. ^{1}H NMR (400 MHz, $CDCl_3$): δ 1.42 [br, 9H, $(CH_3)_3C$—], 2.82 (br, 2H, —CH_2—), 3.70 (br, 3H, —OCH_3), 4.33 (br, 1H, —*CH*—), 5.60–6.42 (br, 2H, —C=C*H*—, —N*H*—). **Poly[(*S*)-1a]**: IR (KBr): 3412, 2980, 2935, 2623, 1704, 1509, 1395, 1369, 1251, 1163, 855 cm^{-1}. ^{1}H NMR (400 MHz, CD_3OD): δ 1.45 [br, 9H, $(CH_3)_3C$—], 2.68 (br, 2H, —CH_2—), 4.23 (br, 1H, —*CH*—), 6.02–6.48 (br, *2*H, —C=C*H*—, —N*H*—). **Poly[(*S*)-4]**: IR (KBr): 3407, 3017, 2949, 1721, 1500, 1450, 1233, 1107, 1075, 739 cm^{-1}. ^{1}H NMR (400 MHz, $CDCl_3$): δ 1.46 (br, 3H, —CH_3), 2.26 (br, 2H, —CH_2—), 3.56 (br, 3H, —OCH_3), 4.01–4.38 (br, 3H, >*CH*—, —CH_2O—), 5.71–5.91 (br, 1H, —N*H*—), 6.29 (br, 1H, —C=C*H*—), 7.12–7.72 (br, 8H, Ar). **Poly[(*S*)-4b]**: IR (in $CHCl_3$): 3438, 3308, 1747, 1714, 1610, 1508, 1424, 1046, 928 cm^{-1}. ^{1}H NMR (400 MHz, $CDCl_3$): δ 1.66 [br, 3H, CH_3—], 2.32 (br, 2H, —CH_2—), 3.75 (br, 3H, —OCH_3), 6.11 (br, 1H, —C=C*H*—).

RESULTS AND DISCUSSION

Polymerization

Rhodium catalysts tolerate a wide variety of functional groups including carbamate and ester, and polymerize monosubstituted acetylenes to afford the corresponding *cis*-stereoregular polymers.[7,8] Thus, the polymerization of monomers (*S*)-/(*R*)-**1**–(*S*)-**4** was carried out using (nbd)Rh$^+$[η^6-$C_6H_5B^-(C_6H_5)_3$] in $CHCl_3$ and THF at 30 °C for 24 h (Scheme 1). The formed polymers were isolated as hexane- or Et_2O-insoluble parts. The polymerization of (*S*)-**1**, (*R*)-**1**, and (*S*)-**4** proceeded homogeneously to give polymers with M_n's of 2400–38,900 in good yields (Table 1). These polymers were soluble in common organic solvents such as $CHCl_3$ and THF. On the other hand, yellow polymeric masses precipitated out of the solution onto the sides of the glass tube in a little while after initiating the polymerization of (*S*)-**2** and (*S*)-**3**. The molecular weights of isolated poly[(*S*)-**2**] and poly[(*S*)-**3**] could not be determined by SEC because they were insoluble in $CHCl_3$, THF, DMF, and H_2O. We further tried the polymerization of (*S*)-**2** and (*S*)-**3** under the conditions different from those in Table 1, but failed to obtain solvent-soluble polymers.[46]

Chiroptical Properties of the Polymers

As shown in Table 1, poly[(*S*)-**1**], poly[(*R*)-**1**], and poly[(*S*)-**4**] displayed $|[\alpha]_D|$ values 5–14 times larger than those of the corresponding monomers, indicating the presence of chirally regulated higher-order structures. The signs of $[\alpha]_D$ of poly[(*S*)-**1**] and poly[(*R*)-**1**], enantiomerically isomeric polymers, were opposite, and the absolute values were almost the same as predicted. The polymers exhibited intense CD signals at the absorption region ranging from 250 to 400 nm in $CHCl_3$, THF, THF/MeOH = 1/1, THF/DMF = 1/1, and DMF as shown in Figures 1 and 2. It is considered that the CD signals originate from chirally arranged chromophors

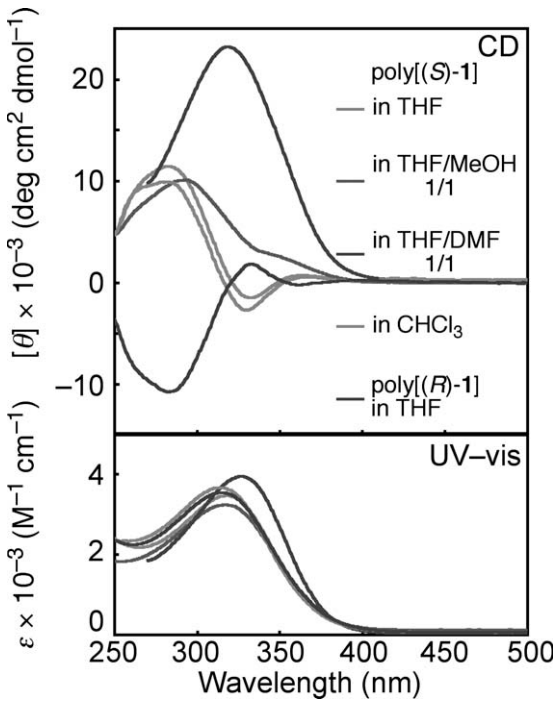

FIGURE 1 CD and UV–vis spectra of poly[(*S*)-**1**] and poly[(*R*)-**1**] measured in $CHCl_3$, THF, THF/MeOH = 1/1, and THF/DMF = 1/1 (c = 0.50 mM) at 20 °C. A color version of this figure is available in the Supporting Information.

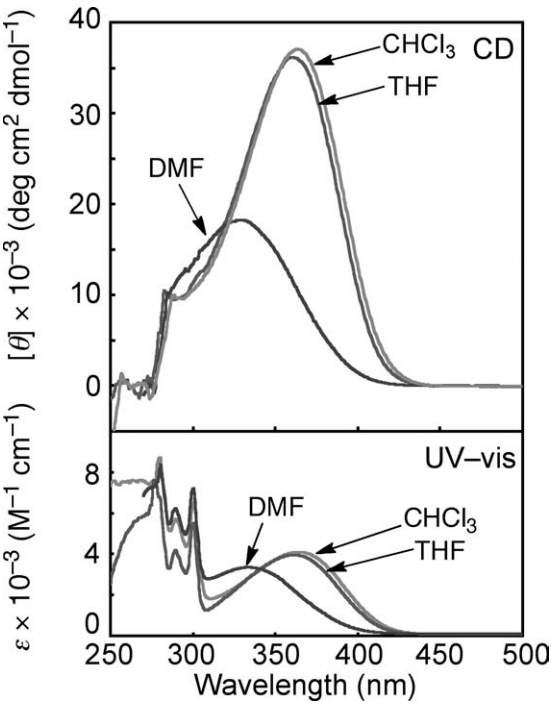

FIGURE 2 CD and UV–vis spectra of poly[(*S*)-**4**] measured in $CHCl_3$, THF, and DMF ($c = 0.50$ mM) at 20 °C.

including conjugated polyacetylene main chain. Fluorine-derived CD signals are negligibly small, presumably because the fluorene moieties are positioned apart from the main chain, which makes their regulated arrangement difficult.[47]

After membrane filtration (pore size = 0.45 μm) of the sample solutions, the CD and UV–vis signals were still observed with the same intensities as those before filtration,[48] and the sample concentration did not affect the signal intensity at a range of 0.25–1.00 mM. These results indicate that the CD signals do not originate from chiral aggregates like the case of poly(thiophene)s[49,50] and poly(*p*-phenylenevinylene)s[50,51] bearing chiral substituents but unimolecular helical conformations of the polymers with predominantly one-handed screw sense.

Poly(*N*-butynylamide)s[15,16] and poly(*N*-propargylamide)s[10,15] efficiently form helices stabilized by intramolecular >N—H ••• O=C< hydrogen bonds between the amide groups at the side chains in nonpolar solvents such as $CHCl_3$. On the other hand, the polymers hardly form helices in polar solvents such as MeOH and DMF, because these solvents disturb the formation of the intramolecular hydrogen bonding. Interestingly, poly[(*S*)-**1**] showed intense CD signals even in THF/MeOH = 1/1 and THF/DMF = 1/1,[52] and the CD intensity of poly[(*S*)-**1**] was larger in THF/DMF = 1/1 than that in less polar THF. Poly[(*S*)-**1**] has high helix-forming ability even in these polar solvents unlike poly(*N*-butynylamide)s and poly(*N*-propargylamide)s. The remarkable helix induction is probably due to the location of stereogenic centers close to the main chain. Namely, it is considered that the presence of chiral groups in close proximities to the main chain is quite effective to induce a helix stabilized by steric repulsion between the side chains, in a fashion similar to poly(1-methylpropargyl alcohol)s,[53] poly(1-methylpropargyl ester)s,[53,54] and poly(1-methylpropargyl-*N*-alkylcarbamate)s.[17] Poly[(*S*)-**1**] and poly[(*R*)-**1**], having side chains with different absolute configurations, exhibited mirror-image CD spectra at 250–500 nm. Together with the results of optical rotations listed in Table 1 {poly[(*S*)-**1**] +113°, poly[(*R*)-**1**] −106°}, it is concluded that these polymers form helical structures with opposite screw sense mutually, and the helix sense is determined by the amino acid chirality. As depicted in Figure 2, poly[(*S*)-**4**] also showed intense CD signals in both nonpolar and polar solvents, $CHCl_3$, THF, and DMF. The UV–vis absorption maximum at the region of main chain chromophore was 33 nm shorter in DMF than those in THF and $CHCl_3$. It is presumed that poly[(*S*)-**4**] form a tightly twisted helix (i.e., smaller pitch/diameter) in DMF than the latter two solvents, causing blue-shift due to the reduced conjugation.[55]

We further examined the thermal stability of helical conformation of the polymers. Figure 3 shows the Kuhn dissymmetry factor ($g = \Delta\varepsilon/\varepsilon$, in which $\Delta\varepsilon = [\theta]/3298$) at $[\theta]_{max}$ of poly[(*S*)-**1**] and poly[(*S*)-**4**] in $CHCl_3$, THF, and DMF at various temperatures. The g value of poly[(*S*)-**1**] decreased 24% by raising temperature from 0 °C to 60 °C in THF, while that of poly[(*S*)-**4**] decreased only 2% under the same temperature range. Since the g values give quantitative information associated with the degree of preferential screw sense,[56] the present results indicate that the helical structure of poly[(*S*)-**4**] is more stable than that of poly[(*S*)-**1**] to thermo-driven screw sense reversal probably due to the larger steric repulsion between the side chains originated from the methyl groups at the chiral centers and bulky fluorenyl groups. The g values of poly[(*S*)-**4**] were smaller and more temperature-sensitive in DMF than those in $CHCl_3$ and THF. In DMF, poly[(*S*)-**4**] may be more flexible than in the latter two solvents, because of the less conjugated main chain as mentioned above. Compared to $CHCl_3$ and THF, it seems that the

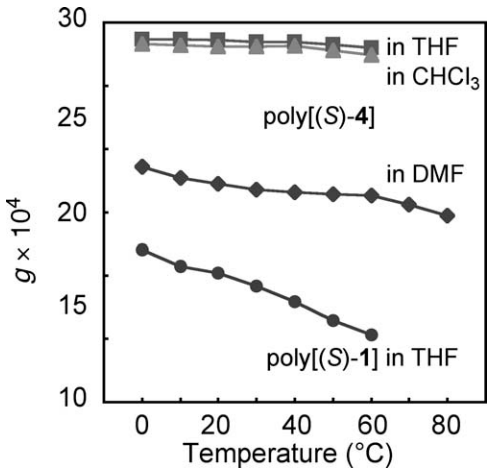

FIGURE 3 Plots of g values of poly[(*S*)-**1**] and poly[(*S*)-**4**] at $[\theta]_{max}$ versus temperature measured in $CHCl_3$, THF, and DMF ($c = 0.50$ mM).

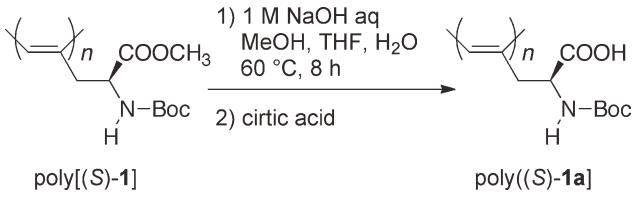

SCHEME 2 Synthesis of poly[(*S*)-**1a**].

solvation ability of DMF with poly[(*S*)-**4**] is high because dipole–dipole interaction between the carbonyl moieties of DMF and the polymer is possibly present along with hydrogen-bonding interaction, resulting in high flexibility of conformation as well.

Removal of Protecting Groups of Poly[(*S*)-1] and Poly[(*S*)-4]

The ester groups of poly[(*S*)-**1**] were hydrolyzed using NaOH aq. to obtain the corresponding polymer {poly[(*S*)-**1a**]} bearing unprotected carboxy groups (Scheme 2).[57] The proceeding of the reaction was confirmed by ^{1}H NMR spectroscopy, i.e., a signal around 3.6–3.8 ppm corresponding to the methyl groups mostly disappeared after hydrolysis.[58] The M_n and M_w/M_n of poly[(*S*)-**1a**] were determined as 30,500 and 1.9 by SEC,[59] respectively, which were almost the same as those of poly[(*S*)-**1**] listed in Table 1. Decomposition during hydrolysis seems to be negligibly small.

Further, removal of the Fmoc groups from poly[(*S*)-**4**] was attempted to obtain poly[(*S*)-**4b**] bearing unprotected amino groups according to Scheme 3. The transformation from poly[(*S*)-**4**] to poly[(*S*)-**4b**] was confirmed by the disappearance of the ^{1}H NMR signals assignable to the Fmoc proton signals. The olefinic proton signal at the main chain was intact.[60] The M_n of poly[(*S*)-**4b**] became low (2100) compared with the precursor {poly[(*S*)-**4**], 7900}. It is considered that this is not due to the decomposition of the main chain but removal of fluorenyl groups, because the M_n of poly[(*S*)-**4b**] calculated based on the MW decrease of fluorenyl groups was 3100, almost the same as the observed one. Another reason may be the formation of amino groups, which commonly extends the retention time of SEC.

Figures 4 and 5 depict the CD and UV–vis spectra of poly[(*S*)-**1a**] and poly[(*S*)-**4b**] measured in THF, MeOH, and DMF. Poly[(*S*)-**1a**] exhibited intense Cotton effects around 300 nm in THF, while only small peaks in MeOH and DMF as shown in Figure 4. Meanwhile, poly[(*S*)-**4b**] exhibited a large minus CD signal around 280 nm both in THF and DMF as shown Figure 5. It is concluded that these polymers bearing

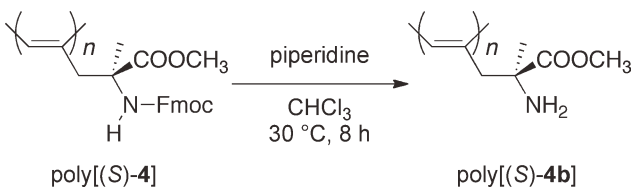

SCHEME 3 Synthesis of poly[(*S*)-**4b**].

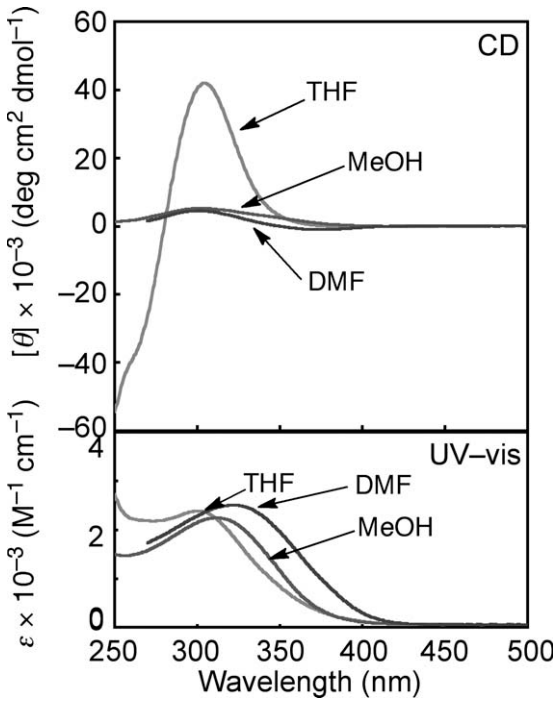

FIGURE 4 CD and UV–vis spectra of poly[(*S*)-**1a**] measured in THF, MeOH, and DMF (c = 0.50 mM) at 20 °C.

unprotected carboxy and amino groups also adopt helical conformations with an excess of predominantly one-handed screw sense in the solvents. It should be noted that CD and UV–vis spectroscopic patterns of poly[(*S*)-**1a**] and poly[(*S*)-**4b**] were totally different from those of the precursors, poly[(*S*)-**1**] and poly[(*S*)-**4**] bearing protected carboxy and amino groups, implying that these polymers form different helical structures before and after removal of the protecting groups. This is predictable because it is likely that the carboxy groups interact with the functional groups at the side chains strongly and intramolecularly, and also with solvent molecules by hydrogen bonding, both of which largely affect the conformation and helicity. This is also the case for amino groups. Specifically, poly[(*S*)-**4b**] exhibited the λ_{max} at a wavelength 30–60 nm shorter than that of poly[(*S*)-**4**]. Removal of bulky Fmoc groups probably reduced the steric repulsion between the side chains, leading to tightening of the helix accompanying the inversion of screw sense as a more stable conformation.

As aforementioned, intramolecular hydrogen bonds possibly exist between the pendent side chains and stabilize the helical structures in a fashion similar to poly(*N*-propargylcarbamate)s[13] and poly(*N*-butynylamide)s.[15,16] Solution-state IR spectroscopic study was carried out under diluted conditions to determine the presence/absence of intramolecular hydrogen bonding. Table 2 summarizes the results of IR measurement for solutions (40 mM)[61] of poly[(*S*)-**1**] and poly[(*S*)-**1a**], and the corresponding monomers (*S*)-**1** and (*S*)-**1a**. Monomer (*S*)-**1** and poly[(*S*)-**1**] exhibited two strong absorption peaks assignable to C=O stretching of ester and carbamate groups, and a peak assignable to N—H bending of the

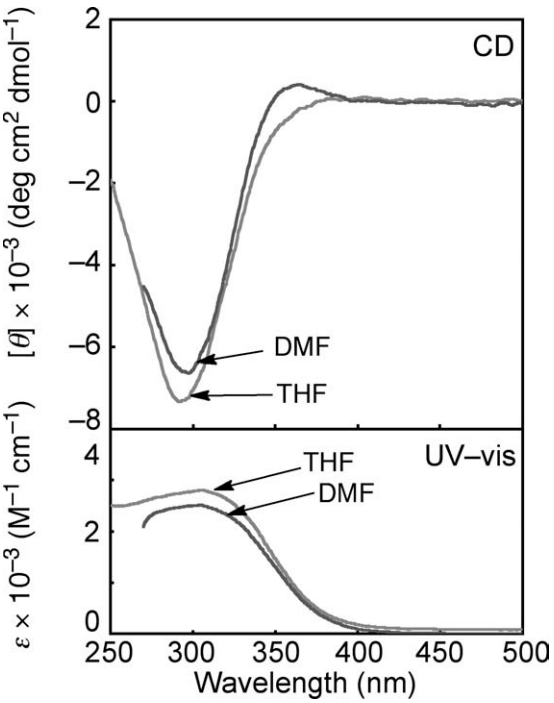

FIGURE 5 CD and UV–vis spectra of poly[(*S*)-**4b**] measured in THF and DMF (c = 0.50 mM) at 20 °C.

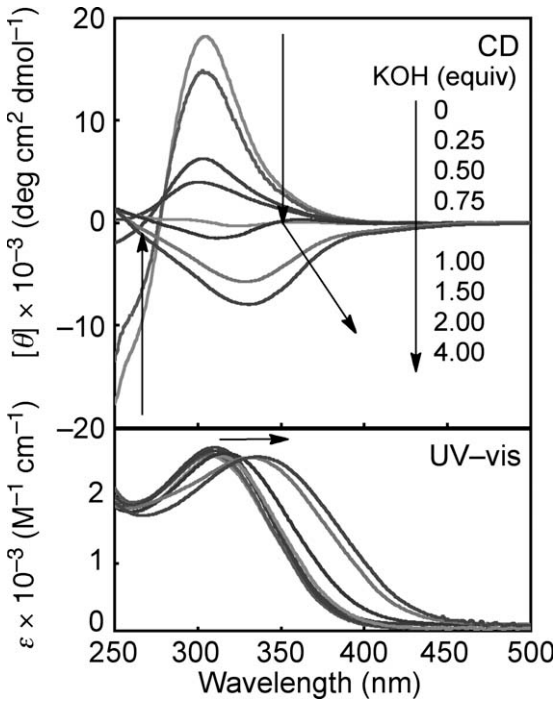

FIGURE 6 CD and UV–vis spectra of poly[(*S*)-**1a**] upon addition of KOH measured in THF/MeOH = 1/1 (c = 0.50 mM) at 20 °C.

carbamate groups. Monomer (*S*)-**1a** and poly[(*S*)-**1a**] exhibited C=O peaks of carboxy groups instead of ester groups. The carbamate C=O peaks of poly[(*S*)-**1**] were observed at 11 cm^{-1} lower, and N—H peaks at 12 cm^{-1} higher wavenumber regions than those of (*S*)-**1**. Compared to the difference of the carbamate C=O peak positions between the monomer and polymer, the difference of ester C=O peak positions was smaller, i.e., 4 cm^{-1}. On the other hand, the difference of carboxy C=O peak positions between (*S*)-**1a** and poly[(*S*)-**1a**] was as large as 16 cm^{-1}. The difference of carbamate C=O peak was 1 cm^{-1} between the monomer and polymer, and that of N—H was 16 cm^{-1}. These results confirm the presence of intramolecular hydrogen bonds in the both polymers, but the patterns seem to be largely different. Namely, it is assumed that poly[(*S*)-**1**] forms intramolecular hydrogen bonds between the C=O and N—H of carbamate groups. The participation of the ester groups in hydrogen bonding of poly[(*S*)-**1**] seems to be negligibly small judging from the trace difference of the ester C=O absorption from that of (*S*)-**1** as mentioned earlier. Meanwhile, poly[(*S*)-**1a**] presumably forms hydrogen bonds between the C=O of unprotected carboxy and N—H of carbamate groups. It is considered that this difference of hydrogen-bonding patterns causes the different helical structures between poly[(*S*)-**1**] and poly[(*S*)-**1a**].

TABLE 2 Solution-State IR Spectroscopic Data (C=O and N—H Absorption Peaks) of the Monomers and Polymers

	Wavenumber (cm^{-1})		
	C=O		
Compound	Ester or carboxy	Carbamate	N—H
(*S*)-**1**[a]	1,746	1,709	1,506
poly[(*S*)-**1**][a]	1,742	1,698	1,518
(*S*)-**1a**[b]	1,747	1,718	1,506
poly[(*S*)-**1a**][b]	1,731	1,717	1,522

[a] Measured in $CHCl_3$ (c = 40 mM).
[b] Measured in THF (c = 40 mM).

Ion Sensing Properties of Poly[(*S*)-1a]

Figure 6 shows the change of CD and UV–vis spectra of poly[(*S*)-**1a**] upon addition of KOH measured in THF/MeOH = 1/1. The CD signal around 250–350 nm gradually decreased by raising the amount of KOH up to 0.75 equiv, and disappeared at 1.00 equiv. Further addition of KOH induced a minus peak around 312 nm at 1.50 equiv, and a red-shift to 330 nm at 4.00 equiv. The analogous spectral change was also observed in MeOH (Supporting Information Fig. S3). It is suggested that poly[(*S*)-**1a**] varied its helical conformation (preference of screw sense and pitch/diameter) in response to KOH in these solvents. The other alkali metal hydroxides were also added to a solution of poly[(*S*)-**1a**]. Figure 7 depicts the CD and UV–vis spectra of poly[(*S*)-**1a**] in the absence and presence of 4 equiv of LiOH and NaOH in THF/MeOH = 1/1, along with the data of KOH. A plus-signed CD signal was observed at 304 nm without an alkali hydroxide, while minus-signed ones were observed around 310–330 nm with all alkali hydroxides. The λ_{max} order was non < LiOH (+23 nm) < NaOH (+2 nm) < KOH (+5 nm).[62] The λ_{max} was more shifted as the size of alkali metal became larger.[63] These results suggest that poly[(*S*)-

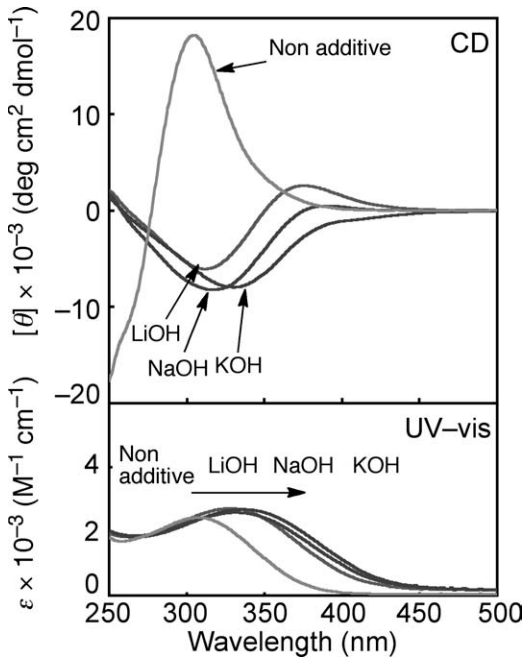

FIGURE 7 CD and UV–vis spectra of poly[(*S*)-**1a**] in the absence and presence of 4 equiv of LiOH, NaOH, and KOH measured in THF/MeOH = 1/1 (c = 0.50 mM) at 20 °C.

1a] changes the structure by the addition of an alkali metal hydroxide due to the ionic interactions between the carboxy groups and cationic species. Since the cations seem to exist close to the carboxy groups of the polymer in THF/MeOH, it is likely that the ionic repulsion between the side chains gets

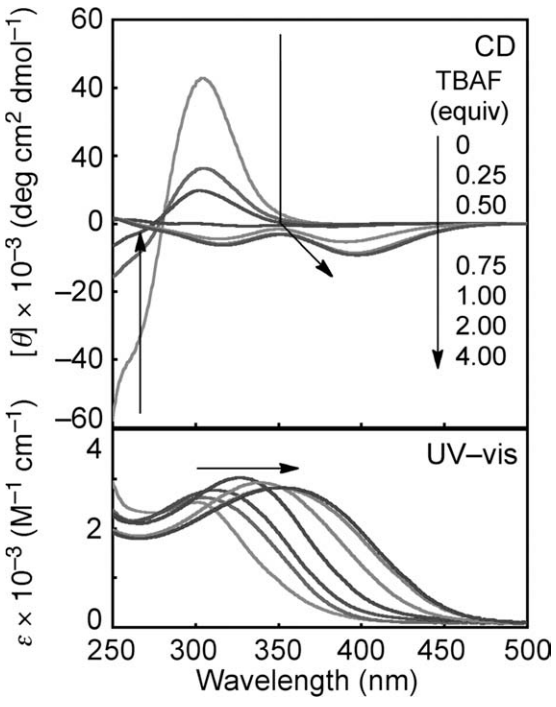

FIGURE 8 CD and UV–vis spectra of poly[(*S*)-**1a**] upon addition of TBAF measured in THF (c = 0.50 mM) at 20 °C.

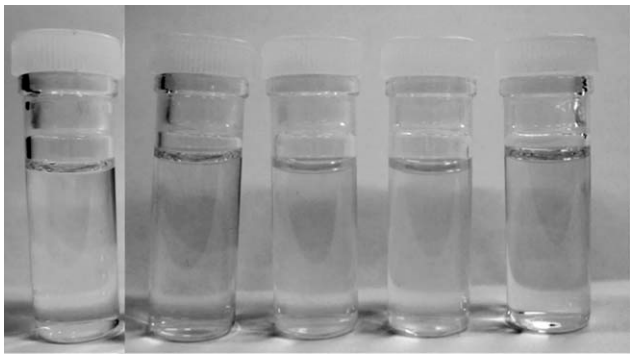

FIGURE 9 Photograph of solutions of poly[(*S*)-**1a**]. From left to right: without additive, with 4 equiv of LiOH, NaOH, KOH measured in THF/MeOH = 1/1, and TBAF measured in THF (c = 0.50 mM). A color version of this figure is available in the Supporting Information.

larger, resulting in a loosely twisted helix (larger pitch/diameter and enhanced conjugation) showing the λ_{max} at a longer wavelength region. Addition of TBAF,[64] which has larger cationic species than the alkali metals,[65,66] was examined in THF. As shown in Figure 8, the CD and UV–vis spectra of poly[(*S*)-**1a**] showed trends similar to those of the case of KOH addition (Fig. 6). The λ_{max} was red-shifted largely by TBAF (51 nm) compared to those by the alkali metal hydroxides (25–30 nm), which supports the assumption of helix-loosening induced by ionic repulsion as mentioned earlier.[67] After the addition of 4 equiv of alkali metal or TBAF to a polymer solution, excess equivalents of HCl was added to the resulting solution. Then the CD and UV–vis spectral patterns completely returned to the original ones. It was confirmed that poly[(*S*)-**1a**] recovered the original helical structure without an alkali metal or TBAF reversibly.[68]

Figure 9 shows the pictures of poly[(*S*)-**1a**] solutions before and after addition of 4 equiv of alkali metal hydroxides and TBAF. Since the color of each polymer solution is distinguishable by the naked eye, the present system may be applicable to an ionic sensor. It is apparent that the ionic interaction between unprotected carboxy groups and additives is the key importance to induce such sensing abilities, because no spectral change was observed upon addition of TBAF to a solution of poly[(*S*)-**1**] bearing protected carboxy groups.

Conformational Analysis

As described earlier, it is considered that the present polymers take predominantly one-handed helical structures. The molecular mechanics calculation (MMFF94[69]) was carried out to gain knowledge on the conformation of the polymers. The conformers of poly[(*S*)-**1**] (18-mer) were optimized with the dihedral angles ϕ at the single bonds in the main chain varying by the increment of 10°. The polymer formed two different patterns of hydrogen bonding according to the value of ϕ, intramolecular hydrogen bonding between *i*th and (i+2)th units, and that between *i*th and (i+3)th units. As shown in Figure 10, a left-handed helical conformer with $\phi = -80°$ was the most stable one. The right-handed

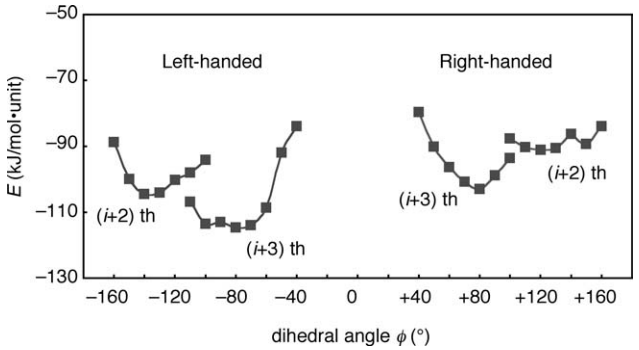

FIGURE 10 Relationship between the dihedral angle at the single bond in the main chain of poly[(*S*)-**1**] (18-mer) and the energy calculated by MMFF94.

counterpart with $\phi = +80^\circ$ was 11.7 kJ/mol unit less stable than the left-handed one. This energy difference between the left- and right-handed helical conformers is explainable by the steric factor. Namely, the van der Waals surface areas of the left- and right-handed conformers with $\phi = -80^\circ$ and $+80^\circ$ are 4663 and 4639 Å^2, and volumes are 3813 and 3813 Å^3, respectively.[70] These data indicate that the left-handed one is more extended, and therefore sterically more favorable than the right-handed one, resulting in the higher stability. The most stable conformer with $\phi = -80^\circ$ forms regulated intramolecular hydrogen-bonding strands between the carbamate groups at *i*th and $(i+3)$th monomer units as depicted in Figure 11. The existence of this pattern of intramolecular hydrogen bonds is supported by the solution-state IR spectroscopic data listed in Table 2.

The conformers of poly[(*S*)-**4**] and poly[(*S*)-**4b**] were also analyzed in a similar fashion to those of poly[(*S*)-**1**]. It is revealed that the most stable conformers of poly[(*S*)-**4**] and poly[(*S*)-**4b**] are left- ($\phi = -80^\circ$) and right-handed ($\phi = +80^\circ$) helices (Supporting Information Fig. S8). These molecular mechanics calculation results well explain the CD signals with opposite sign of these two polymers.

CONCLUSIONS

In the present study, we have demonstrated the synthesis and polymerization of novel optically active substituted acetylenes (*S*)-/(*R*)-**1**–(*S*)-**4** derived from α-propargylglycine and α-propargylalanine using a rhodium zwitterionic catalyst. Poly[(*S*)-**1**], poly[(*R*)-**1**], and poly[(*S*)-**4**] exhibited optical rotations 5–14 times larger than those of the corresponding monomers. These polymers showed intense CD signals at the absorption region of the conjugated polyacetylene backbone. Since the CD patterns and intensities were not affected by membrane filtration and sample concentration, the chiroptical properties are not explainable by the formation of chiral aggregates but predominantly one-handed helical structures. As far as we know, this is the first example regarding the synthesis of α-propargyl amino acid-derived helical polyacetylenes. Removal of the protecting groups from poly[(*S*)-**1**] and poly[(*S*)-**4**] provided poly[(*S*)-**1a**] and poly[(*S*)-**4b**] bearing unprotected carboxy and amino groups, respectively. The helical natures of poly[(*S*)-**1a**] and poly[(*S*)-**4b**] were largely different from those of the precursor polymers, presumably due to the participation of carboxy and amino groups into intramolecular hydrogen-bonding strands at the side chains, which play an important role for helix formation and stabilization. The presence of intramolecular hydrogen bonding is supported by the shifts of C=O and N—H IR absorption to lower and higher wavenumber regions from monomers to polymers. The different patterns of hydrogen bonding of poly[(*S*)-**1**] and poly[(*S*)-**1a**] is also suggested by IR spectroscopy. The helical structure of poly[(*S*)-**1a**] became extended upon addition of alkali hydroxides (LiOH, NaOH, and KOH) and TBAF, and the degree of extension agreed with the order of the cation size, which were confirmed by the red λ_{max} shift of the CD and UV–vis peaks. A conceivable idea for explaining this phenomenon is the change of ionic and steric repulsion between the side chains. Namely, the repulsion becomes large due to the cations existing close to the carboxylate moieties, resulting in helix loosening accompanying the extension of conjugation of the polyacetylene backbone, and the order of the red-shift agrees with that of cation size. Poly[(*S*)-**1a**] has potential as a cation sensor since the ion-responsive conformational transition is reversible and causes the color change of the polymer solution detectable by the naked eye. Molecular mechanics calculation suggested that the most stable conformer of poly[(*S*)-**1**] was a left-handed helix stabilized by intramolecular hydrogen bonds between the carbamate groups, whose presence was confirmed by IR spectroscopy as mentioned. Further investigation on the mechanistic aspects of conformational change of poly[(*S*)-**1a**] upon addition

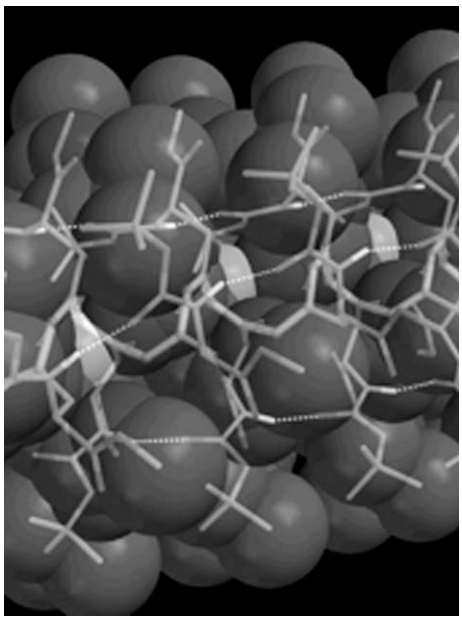

FIGURE 11 The most stable conformer of poly[(*S*)-**1**] optimized by MMFF94. The dihedral angles ϕ at the single bonds in the main chain are -80°. The green dotted lines represent hydrogen bonds between the carbamate groups at *i*th and $(i+3)$th monomer units. The polyacetylene backbone is colored in yellow. A color version of this figure is available in the Supporting Information.

of alkali metal and TBAF with considering solvent effect, and responsiveness of poly[(S)-**4b**] bearing unprotected amino groups to various acids are now under progress.

This research was supported by the Kyoto University Global COE Program "International Center for Integrated Research and Advanced Education in Materials Science" from the Ministry of Education, Culture, Sports, Science, and Technology, Japan, and The Sumitomo Foundation, and Nagase & Co., Ltd.

REFERENCES AND NOTES

1 For a review, see: Nakano, T.; Okamoto, Y. *Chem. Rev.* **2001,** *101*, 4013–4038.

2 For a review, see: Amabilino, D. B.; Serrano, J.; Sierra, T.; Veciana, J. *J. Polym. Sci. Part A: Polym. Chem.* **2006,** *44*, 3161–3174.

3 For a review, see: Sato, T.; Terao, K.; Teramoto, A.; Fujiki, M. *Polymer* **2003,** *44*, 5477–5495.

4 For a review, see: Hill, D. J.; Mio, M. J.; Prince, R. B.; Hughes, T. S.; Moore, J. S. *Chem. Rev.* **2001,** *101*, 4013–4018.

5 For a review, see: Masuda, T. *J. Polym. Sci. Part A: Polym. Chem.* **2007,** *45*, 165–180.

6 Natta, G.; Pino, P.; Corradini, P.; Danusso, F.; Manititca, E.; Nazzanti, G.; Moraglio, G. *J. Am. Chem. Soc.* **1955,** *77*, 1708–1710.

7 Tabata, M.; Yang, W.; Yokota, K. *Polym. J.* **1990,** *22*, 1105–1107.

8 Kishimoto, Y.; Eckerle, P.; Miyatake, T.; Kainosho, M.; Ono, A.; Ikariya, T.; Noyori, R. *J. Am. Chem. Soc.* **1999,** *121*, 12035–12044.

9 Ke, Z.; Abe, S.; Ueno, T.; Morokuma, K. *J. Am. Chem. Soc.* **2011,** *133*, 7926–7941.

10 Nomura, R.; Tabei, J.; Masuda, T. *J. Am. Chem. Soc.* **2001,** *123*, 8430–8431.

11 Tabei, J.; Nomura, R.; Masuda, T. *Macromolecules* **2002,** *35*, 5405–5409.

12 Tabei, J.; Nomura, R.; Masuda, T. *Macromolecules* **2003,** *36*, 573–577.

13 Nomura, R.; Nishiura, S.; Tabei, J.; Sanda, F.; Masuda, T. *Macromolecules* **2003,** *36*, 5076–5080.

14 Sanda, F.; Nishiura, S.; Shiotsuki, M.; Masuda, T. *Macromolecules* **2005,** *38*, 3705–3078.

15 Tabei, J.; Shiotsuki, M.; Sanda, F.; Masuda, T. *Macromolecules* **2005,** *38*, 5860–5867.

16 Suzuki, Y.; Tabei, J.; Shiotsuki, M.; Inai, Y.; Sanda, F.; Masuda, T. *Macromolecules* **2008,** *41*, 1086–1093.

17 Shirakawa, Y.; Suzuki, Y.; Terada, K.; Shiotsuki, M.; Masuda, T. *Macromolecules* **2010,** *43*, 5575–5581.

18 Sanda, F.; Araki, H.; Masuda, T. *Macromolecules* **2004,** *37*, 8510–8516.

19 Zhao, H.; Sanda, F.; Masuda, T. *Macromolecules* **2004,** *37*, 8888–8892.

20 Gao, G.; Sanda, F.; Masuda, T. *Macromolecules* **2003,** *36*, 3932–3937.

21 Zhao, H.; Sanda, F.; Masuda, T. *Macromolecules* **2004,** *37*, 8893–8896.

22 Sanda, F.; Araki, H.; Masuda, T. *Macromolecules* **2005,** *38*, 10605–10608.

23 Cheuk, K. K. L.; Li, B. S.; Lam, J. W. Y.; Xie, Y.; Tang, B. Z. *Macromolecules* **2008,** *41*, 5997–6005.

24 Maeda, K.; Kamiya, N.; Yashima, E. *Chem.—Eur. J.* **2004,** *10*, 4000–4010.

25 Sanda, F.; Terada, K.; Masuda, T. *Macromolecules* **2005,** *38*, 8419–8154.

26 Liu, R.; Sanda, F.; Masuda, T. *Polymer* **2007,** *48*, 6510–6518.

27 Chan, K. H.; Lam, J. W.; Wong, K. M.; Tang, B. Z.; Yam, V. W. *Chem.—Eur. J.* **2009,** *15*, 2328–2334.

28 Zheng, Y.; Cui, J.; Zheng, J.; Wan, X. *J. Mater. Chem.* **2010,** *20*, 5915–5922.

29 Sanda, F.; Teraura, T.; Masuda, T. *J. Polym. Sci. Part A: Polym. Chem.* **2004,** *42*, 4641–4647.

30 Zhao, H.; Sanda, F.; Masuda, T. *Polymer* **2006,** *47*, 2596–2602.

31 Kakuchi, R.; Nagata, S.; Tago, Y.; Sakai, R.; Otsuka, I.; Satoh, T.; Kakuchi, T. *Macromolecules* **2009,** *42*, 1476–1481.

32 Kakuchi, R.; Tago, Y.; Sakai, R.; Satoh, T.; Kakuchi, T. *Macromolecules* **2009,** *42*, 4430–4435.

33 Louzao, I.; Seco, J. M.; Quiñoá, E.; Riguera, R. *Angew. Chem. Int. Ed.* **2010,** *49*, 1430–1433.

34 Sakai, R.; Sakai, N.; Satoh, T.; Li, W.; Zhang, A.; Kakuchi, T. *Macromolecules* **2011,** *44*, 4249–4257.

35 Liu, R.; Sanda, F.; Masuda, T. *J. Polym. Sci. Part A: Polym. Chem.* **2008,** *46*, 4175–4182.

36 Sanda, F.; Araki, H.; Masuda, T. *Chem. Lett.* **2005,** *34*, 1642–1643.

37 Maeda, K.; Tanaka, K.; Morino, K.; Yashima, E. *Macromolecules* **2007,** *40*, 6783–6785.

38 Terada, K.; Masuda, T.; Sanda, F. *J. Polym. Sci. Part A: Polym. Chem.* **2009,** *47*, 4971–4981.

39 Ikeda, A.; Terada, K.; Shiotsuki, M.; Sanda, F. *J. Polym. Sci. Part A: Polym. Chem.* **2011,** *49*, 3783–3796.

40 Sanda, F.; Gao, G.; Masuda, T. *Macromol. Biosci.* **2004,** *4*, 570–574.

41 Terada, K.; Masuda, T.; Sanda, F. *Macromolecules* **2009,** *42*, 913–920.

42 Ohsawa, S.; Sakurai, S.; Nagai, K.; Banno, M.; Maeda, K.; Kumaki, J.; Yashima, E. *J. Am. Chem. Soc.* **2011,** *133*, 108–114.

43 For a review, see: Maruoka, K. *Bull. Chem. Soc. Jpn.* **2009,** *82*, 917–930.

44 Walensky, L. D.; Kung, A. L.; Escher, I.; Malia, T. J.; Wright, R. D.; Wagnew, G.; Verdine, G. L.; Korsmeyer, S. J. *Science* **2004,** *305*, 1466–1470.

45 Schrock, R. R.; Osborn, J. A. *Inorg. Chem.* **1970,** *9*, 2339–2343.

46 The more detail about the polymerization results is listed in Table S1 in the Supporting Information.

47 In the case of poly[(*S*)-**4**], fluorine-derived absorption peaks exist at 250–300 nm, shorter than the wavelength region of polyacetylene backbone.

48 It has been reported that membrane filtration of solutions of conjugated polymers is effective to remove aggregates. See Yamamoto, T.; Komarudin, D.; Arai, M.; Lee, B.-L.; Suganuma, H.; Asakawa, N.; Inoue, Y.; Kubota, K.; Sasaki, S.; Fukuda, T.; Matsuda, H. *J. Am. Chem. Soc.* **1998,** *120*, 2047–2058.

49 Yue, S.; Berry, G. C.; McCullough, R. D. *Macromolecules* **1996,** *29*, 933–939.

50 Langeveld-Voss, B. M. W.; Peeters, E.; Janssen, R. A. J.; Meijer, E. W. *Synth. Met.* **1997,** *84*, 611–614.

51 Peeters, E.; Janssen, R. A. J.; Meijer, E. W. *Synth. Met.* **1999,** *102*, 1105–1106.

52 Poly[(*S*)-**1**] and poly[(*R*)-**1**] were insoluble in MeOH and DMF.

53 Suzuki, Y.; Shiotsuki, M.; Sanda, F.; Masuda, T. *Macromolecules* **2007,** *40*, 1864–1867.

54 Suzuki, Y.; Shiotsuki, M.; Sanda, F.; Masuda, T. *Chem. Asian J.* **2008,** *3*, 2075–2081.

55 Percec, V.; Obata, M.; Rudick, J. G.; De, B. B.; Glodde, M.; Bera, T. K.; Magonov, S. N.; Balagurusamy, V. S. K.; Heiney, P. A. *J. Polym. Sci. Part A: Polym. Chem.* **2002,** *40*, 3509–3533.

56 Fujiki, M. *Macromol. Rapid Commun.* **2001,** *22*, 539–563.

57 We also tried to obtain poly[(*S*)-**1a**] by the polymerization of (*S*)-**1a** bearing unprotected carboxy groups, but failed under the conditions in Table 1, presumably due to the deactivation of the rhodium catalyst by the carboxy groups. See Saito, M. A.; Maeda, K.; Onouchi, H.; Yashima, E. *Macromolecules* **2000,** *33*, 4616.

58 See the ^{1}H NMR spectra of the polymers before and after hydrolysis (Fig. S1).

59 The carboxy groups were transformed into methyl ester groups using trimethylsilyldiazomethane, because poly[(*S*)-**1a**] was not eluted out.

60 See the ^{1}H NMR spectra of the polymers before and after deprotection (Fig. S2).

61 This concentration is low enough to eliminate the effect of intermolecular hydrogen bonding.

62 RbOH was hardly soluble in THF/MeOH = 1/1. CsOH (4 equiv) shifted the λ_{max} but induced no clear CD signal unlike the others. See Figure S4.

63 Ionic radius (Å): Li^+ 0.9, Na^+ 1.2, K^+ 1.5. See Shannon, R. D. *Acta. Cryst. 1976*, A32, 751–767.

64 Addition of tetrabutylammonium hydroxide was also examined but the trends of CD and UV–vis spectra were different from those with alkali metal hydroxides (Fig. S5).

65 The ionic radius of Bu_4N^+ = 4.8 Å. See Watanabe, Y.; Ohnaka, K.; Fujita, S.; Kishi, M.; Yuchi, A. *Anal Chem* **2011,** *83*, 7480–7485.

66 Mo, H.; Pochapsky, T. C. *J. Phys. Chem. B* **1997,** *101*, 4485–4486.

67 No red-shift of λ_{max} was observed upon TBAF addition in THF/MeOH = 1/1 and THF/H_2O= 1/1 (Supporting Information Fig. S6). The ionic interaction between unprotected carboxy groups and TBAF does not seem preferable in highly polar solvents, presumably due to the presence of hydrophobic alkyl groups.

68 See the CD and UV–vis spectra of poly[(*S*)-**1a**] with 100 equiv of HCl after addition of 4 equiv of KOH in THF/MeOH (Fig. S7). We could not examine the possibility of proton extraction from the polymer main chain or side groups by ^{1}H NMR spectroscopy after alkali addition, because the polymer concentration was too low to measure the NMR spectra. Proton extraction reactions from vinylene and carbamate are commonly carried out using alkyl lithium and NaH, whose basicities are much higher than those of alkali hydroxides. TBAF also strongly affected the CD and UV–vis spectra of the polymer in a fashion similar to alkali hydroxides, although the basicity of TBAF is much lower than those of alkali hydroxides. It is therefore likely that the interaction between the carboxy groups and ions caused the conformational changes as mentioned. We can deny the cis-trans isomerization of the double bonds at the main chain after the addition of alkali hydroxides since the CD and UV–vis spectral patterns completely returned to the original ones by the addition of HCl. We assume that the chirotopic change is mainly brought about by the change of population of right and left handed helices as well as change of degree of twisting.

69 Halgren, T. A. *J. Comput. Chem.* **1996,** *17*, 490–519. The molecular mechanics calculation was carried out with Wavefunction Inc., Spartan '10 Macintosh.

70 Calculated by Winmostar Ver. 3.8. http://winmostar.com/; Senda, N. *Idemitsu Tech. Rep.* **2006,** *49*, 106–111.